ChemComm

FEATURE ARTICLE

View Article Online
View Journal | View Issue

Cite this: *Chem. Commun.*, 2023, **59**, 13820

Chemical synthesis of complex oxide thin films and freestanding membranes

Pol Salles, † Pamela Machado,† Pengmei Yu and Mariona Coll *

Oxides offer unique physical and chemical properties that inspire rapid advances in materials chemistry to design and nanoengineer materials compositions and implement them in devices for a myriad of applications. Chemical deposition methods are gaining attention as a versatile approach to develop complex oxide thin films and nanostructures by properly selecting compatible chemical precursors and designing an accurate cost-effective thermal treatment. Here, upon describing the basics of chemical solution deposition (CSD) and atomic layer deposition (ALD), some examples of the growth of chemically-deposited functional complex oxide films that can have applications in energy and electronics are discussed. To go one step further, the suitability of these techniques is presented to prepare freestanding complex oxides which can notably broaden their applications. Finally, perspectives on the use of chemical methods to prepare future materials are given.

Received 23rd June 2023,
Accepted 16th October 2023

DOI: 10.1039/d3cc03030j

rsc.li/chemcomm

1 Transition metal complex oxides

Transition metal complex oxides are a rich family of compounds presenting extraordinary physical phenomena ranging from superconductivity, multiferroicity, magnetism, catalytic activity to simultaneous optical transparency and conductivity.[1,2] They also offer high stability with the possibility to work with low-toxic and abundant elements holding great potential to outperform conventional materials for many applications. Consequently, these complex oxides have raised enormous interest to be integrated in next-generation electronic devices envisaging distinct and novel properties that can deliver unprecedented performance improvement.[3] Their crystalline structure, phase and orientation play an essential role in their properties and ultimately define their functionality. A typical way to control the crystallinity of thin films and heterostructures is through the epitaxial growth on single crystal oriented materials. The properties of these crystalline oxide films are strongly dependent on the presence of defects such as off-stoichiometry, structural distortions, strain, and the formation of interfaces with precise configuration[4–6] which in turn depend on the synthesis process

Institut de Ciència de Materials de Barcelona (ICMAB-CSIC) Campus UAB, 08193 Bellaterra (Barcelona), Spain. E-mail: mcoll@icmab.es; Tel: +34 935801853
† These authors contributed equally to this work.

Pol Salles

Pol Salles got his PhD in Materials Science at the Universitat Autonoma de Barcelona, UAB (ICMAB-CSIC, 2019–2023). He obtained his BSc in Nanoscience and Nanotechnology at the Autonomous University of Barcelona in 2015 and his MSc in Materials for Energy Storage and Conversion (MESC) in 2018 in between several universities at France, Poland and USA. His research focuses on the development of chemical synthesis methods to prepare freestanding thin films of epitaxial complex oxide for electronics and energy applications.

Pamela Machado

P. Machado received her BS degree in Nanoscience and Nanotechnology from the Universitat Autònoma de Barcelona (UAB), Spain in 2016, followed by her MS in Applied Materials Chemistry from the University of Barcelona in 2017. She has been working at ICMAB-CSIC for five years, where she received her PhD in Material Science from UAB in 2023. Her research focuses on the preparation of multifunctional oxide thin films with engineered properties for energy applications, prioritizing the use of versatile and cost-effective solution-based deposition techniques.

of the complex oxides. Pulsed laser deposition (PLD),[7,8] molecular beam epitaxy (MBE)[9,10] and hybrid growth[11] have demonstrated the feasibility to prepare high quality complex oxide crystalline films. When evaluating the suitability of an oxide material it is important to consider cost-effective and sustainable processing techniques. Over the past decades, significant progress has been made to enable the production of high quality metal oxide thin films using chemical solution deposition, also named solution processing (CSD) and atomic layer deposition (ALD). These emerging thin film growth techniques, both inexpensive and potentially scalable, offer the possibility to prepare epitaxial oxides and perform demanding compositional tuning by identifying thermally and chemically compatible metalorganic precursors.[12–14] The study of the thermal decomposition of the precursors and the influence of the processing parameters to the oxide conversion mechanism have been essential to progress towards enlarging the library of complex oxides prepared by chemical methods.[15,16] Yet, challenges remain on the synthesis level to accurately prepare and nanoengineer many more complex oxides to meet the demands of todays advanced materials. In this vein, the development of strategies that allow detaching the complex oxide from the growth substrate and freely manipulate them allowed identifying exotic properties. This opened a new ground of research including stacking heterostructures and superlattices not achievable by simple epitaxial growth[17,18] and extend them to bendable, wearable and light-weight devices.[19,20] Here, the use of chemical deposition methodologies to fabricate these materials can also offer new opportunities.

In this feature article the distinctive characteristics of CSD and ALD are briefly introduced followed by the presentation of some examples developed in our group of successful deposition of complex oxide thin films on rigid substrates with increased composition intricacy ($BiFeO_3$, $Bi_{1-y}La_yFe_{1-x}Co_xO_3$, $La_{0.75}Cr_{0.25}MnO_3$, Co_2FeO_4 and $Gd_xFe_yO_z$). Finally the main challenges to prepare freestanding complex oxides by chemical methods ($CoFe_2O_4$ and $La_{0.7}Sr_{0.3}MnO_3$) are reviewed.

2 Chemical deposition methods: solution processing and atomic layer deposition

The growth of complex oxide thin films by CSD and ALD starts from an appropriate selection of chemical precursors that, upon its combination with compatible solvents in the case of CSD or volatilized in the case of ALD, are deposited on a substrate and subsequently converted to crystalline oxides after being exposed to a thermal treatment. It is worth noting that the use of chemical precursors allows to easily tune film composition and stoichiometry.

For CSD, the chemical reactants are mixed in a stoichiometric ratio according to the final film composition. The selection of the appropriate solvent (polarity, protic/aprotic...), ligand chemistry (tether, length, bulky...) and the use of complexing agents (amines, acetylacetone...) help design the optimal solution formulation to ensure a homogeneous deposition (viscosity, surface tension) and controlled kinetics for clean decomposition.[12,13,21] The most commonly adopted deposition methods are spin-coating, dip-coating, slot-die coating, ink-jet printing and spray pyrolysis. After deposition, film drying and decomposition of the organic components occur at low temperature. The processing temperature, atmosphere, time, heating/cooling rates enable to control this decomposition and the conversion process by guiding the evolution of the intermediate species, cation distribution, densification, formation of defects, and ultimately the crystallization of the oxide phase (see Fig. 1).[16] When epitaxy is pursued the selection of a lattice matched substrate, which sometimes can be challenging, is also a crucial step for the oxide synthesis.[22]

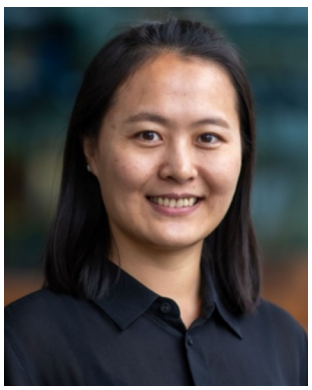

Pengmei Yu

Pengmei Yu received her PhD degree in 2020 in Materials Science at Universitat Autònoma de Barcelona, Spain for her work at Institute of Materials Science of Barcelona. Her research was dedicated to the ALD of functional transition metal oxide thin films and the nanoengineering of transition metal oxides–carbon nanocomposites interface chemistry. Afterwards, she joined the Plasma Materials and Processing group at Technische Universiteit Eindhoven as a Postdoctoral researcher, where she focused on the mechanistic studies on area-selective ALD processes for electronic applications enabled by small molecule inhibitors.

Mariona Coll

Mariona Coll graduated in Chemistry at the Universitat de Barcelona and holds a PhD in Materials Science from Universitat Autònoma de Barcelona. She was a postdoctoral researcher at the University of Maryland and NIST (USA) for 3 years. At present, she is a tenured Scientist at ICMAB-CSIC, Spain. Her current research interests include the synthesis and characterization of functional oxide thin films and nanostructures with engineered properties combining nanochemistry and cost effective deposition methodologies, that can be used for energy and electronic applications.

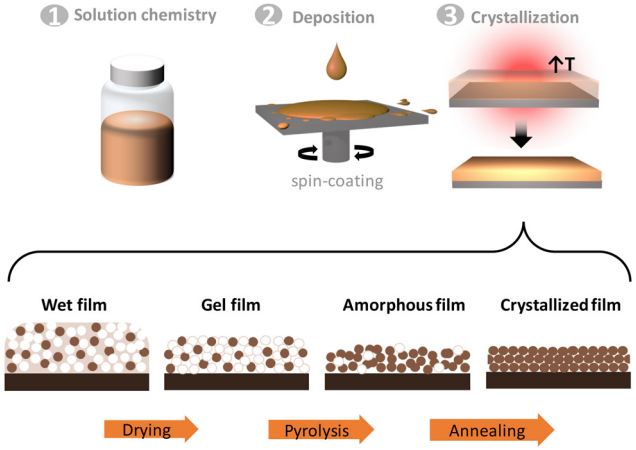

Fig. 1 Sketch of the CSD process including the preparation of the solution chemistry, deposition and crystallization. The latter involves the conversion of the wet film to a crystalline film using thermal treatment.

The preparation of crystalline complex oxides by CSD usually requires temperatures ranging between 400 °C and 900 °C. Significant progress has been made on developing strategies to decrease the processing temperature aiming for a more budget-friendly approach and the possibility to work on temperature-sensitive substrates. In this spirit, the use of photosensitive ligands that can be decomposed using light instead of temperature, the self-combustion method, plastic transfer techniques or a selection of substrates with appropriate interface energy bring higher versatility to the solution methodology being compatible with traditional amorphous semiconductor substrates and flexible electronics.[23–25] Appropriate control of the solution concentration, chemistry and deposition conditions permit to modify the film thickness. For example, using multideposition few millimeter thick single phase complex oxide films can be obtained.[26,27] On the other hand, by means of ink-jet printing, micrometer-lateral size pitches of 1 mm thick films can be prepared by a single deposition.[28] Remarkably, the flexibility that solution processing offers in terms of chemical formulation enables the preparation of more complex systems such as nanocomposites. It was demonstrated that two different functional oxides can be spontaneously crystallized from a single metal organic solution delivering films with enhanced performance compared to the individual parts.[29] An attractive approach to gain further control of the nanocomposite oxide phases and sizes is to add pre-formed nanoparticles in the precursor solution.[30,31] It is worth noting that CSD also allows preparation of complex oxide nanostructures by means of nanoporous polymeric templates[32] and self-assembled nanostructures based on strain engineering.[33]

On the other hand, ALD is a chemical deposition method with unrivaled uniformity and conformality due to its unique self-limiting surface reaction mechanism. Its unprecedented excellence includes atomic-scale control over the composition and thickness, superior ability in tuning and engineering interfaces, and potential compatibility with other production steps thanks to its mild processing conditions.[34] In temporal

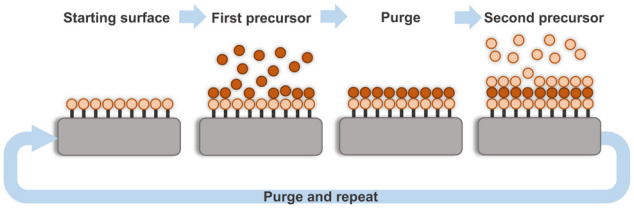

Fig. 2 Sketch of an ALD process identifying the sequential pulse of the precursors separated by purging steps and repeated in a cyclic manner.

ALD the gas-phase precursors are alternately pulsed in the reaction chamber interleaved by purging steps under vacuum conditions and at relatively low temperature (<300 °C), see Fig. 2. The reaction kinetics in ALD depend on several parameters including the precursor chemistry, precursor size and gas flow which will clearly determine the precursor sticking possibility to specific substrate site, architecture and reactor type (temporal *vs.* spatial), and therefore they will define the deposition regime (diffusion or reaction). At the same time, the deposition temperature will also influence the reaction mechanism and growth rate which will ultimately determine the film thickness.[35–38] The ALD processing conditions favor the formation of amorphous or polycrystalline films although the chemistry of the precursor and the processing time can contribute to obtain crystalline and even epitaxial films (using appropriate substrate) at lower temperature. Otherwise, post annealing at high temperature helps achieve a specific degree of crystallinity. Beyond the preparation of thin films, the precise control and high step coverage of ALD enables the preparation of elaborate nanostructures either by area selective deposition and atomic etching[39,40] or conformal coating of nanostructured and porous templates.[41,42] Additionally, dedicated reactors such as roll-to-roll, batch and spatial ALD allow to obtain large and homogeneous coatings.[35,37,43,44]

Unsurprisingly, oxide materials are one of the most studied classes of materials synthesized by ALD.[45–48] Accurate control of precursor pulses, sequence ratio and supercycles[14,47,49] is mandatory to fine tune the stoichiometry and minimize the formation of secondary phases.[50–54] Additionally, identifying thermodynamically and chemically compatible precursors under the same deposition conditions is not an easy task, especially for multication oxides.[55] To simplify this scenario, there is a growing field on the use of single-source heterobimetallic precursors.[56–58] In these precursors, two or more metal elements are included in the molecular structure, thus rendering them very appealing for the preparation of complex oxides by ALD.[59] Another feature that contributes to process intricacy is the fact that the film surface changes constantly with precursor pulses making the system become a non-equilibrium state. During the process, the surface morphology, chemistry and surface area can be easily altered along with the material growth rate, which is exclusively severe in the case of multication material synthesis where sometimes the formation of binary oxides is preferred. Therefore, when precursors with novel chemistries are evaluated or two or more precursors of unknown reactivity are combined,

Table 1 Comparison of benefits, challenges and aims of CSD and ALD as deposition techniques to prepare complex oxides

	Benefits	Challenges and aims
CSD	• Versatility of compositions by mixing stoichiometric amounts of chemical precursors	• Achieve angstrom-scale roughness
	• Epitaxy in thin films (>500 °C)	• Improve control of defect density
	• Micrometer thick films demonstrated	• Homogeneity in large areas *via* slot-die coating, dip coating
	• Versatility to prepare nanocomposites (size, distribution, crystallinity)	• Decrease growth temperature through UV-light sensitive precursors/self-combustion
	• Nanostructures by means of the use of polymer template or interfacial strain	• Develop new chemistries to broaden the material composition range
	• Minimum initial investment (no vacuum)	
ALD	• Precise control of the thickness and composition at an atomic level in simple compositions	• Improve stoichiometry control in complex compositions
	• Thin (<300 nm) and ultrathin films	• Develop new chemistries
	• Conformal coating (3D and complex architectures, nanoparticles)	• Extend area selective deposition/etching from binary to complex oxides
	• Sharp interface	• Improve deposition rate in thick and complex composition films
	• Low T processing and epitaxy (<300 °C)	• Batch and roll-to-roll, spatial ALD for large area and homogeneous deposition
	• Optimized precursor dose	

they represent an imperative challenge for the researcher to develop the deposition process and requires detailed study of the precursor adsorption and surface reactions to obtain uniform growth with controlled film stoichiometry.[60,61] In view of all the above information, cautious design and fine-tuning of the chemical structures of novel precursors offer great opportunities to synthesize and engineer simple and complex oxide systems.

As a summary, Table 1 lists the benefits and challenges of ALD and CSD.

3 Complex oxides on rigid substrates

In this section we will present four different examples of complex oxides prepared by chemical deposition methods on rigid substrates developed in our group. The focus is on the opportunities and intricacies of ALD and CSD to obtain high quality epitaxial films with atomic control.

$BiFeO_3$ (BFO) has attracted great interest as a room temperature multiferroic material.[62] In the last ten years, it gained attention for use in photovoltaic (PV) devices owing to its relatively small band gap (2.7 eV) and the bulk photovoltaic effect.[63,64] The preparation of epitaxial BFO thin films has been reported to be challenging. First, from a thermodynamic standpoint the formation of $Bi_{25}FeO_{39}$ and $Bi_2Fe_4O_9$ secondary phases are favorable over $BiFeO_3$.[65–67] Then, the different evaporation tendency of Bi *versus* Fe makes the formation of defects (*i.e.* oxygen vacancies) complicated to control.[68,69] Finally, the reaction kinetics, which depend on the synthetic process (ALD, PLD, CSD) and purity of the precursors can also promote the formation of specific defects and secondary phases.[65,70–72] The mild deposition conditions of ALD could prevent some of these issues. Few studies on the synthesis of epitaxial BFO by ALD have been reported, mainly because of the poor availability of compatible precursor chemistries.[73,74] In our group we have investigated the preparation of ALD-BFO by alternate pulsing of commercially available and chemically dissimilar bismuth tris(2,2,6,6-tetramethyl-3,5-heptadionate) [$Bi(thd)_3$] and ferrocene [$Fe(Cp)_2$] combined with ozone at 250 °C on (001) $SrTiO_3$ (STO) single crystal substrates. To ensure that the Bi : Fe 1 : 1 cation ratio was achieved minimizing Bi volatilization, the ALD process ended with Fe–O cycles.[72,75] Nanocrystalline and weakly ferroelectric films were obtained in the as-deposited stage that evolved into a (00l)-oriented film showing robust ferroelectricity with an optical bandgap at 2.7 eV after annealing at 650 °C.[75] Nonetheless, (110)-oriented grains were also detected in the final film which are probably formed because of the distinct precursor chemistry that leads to non-optimal reactivity and thermal compatibility.[76–78]

The use of solution processing to prepare BFO films is a solid alternative in which epitaxial and polycrystalline films have been successfully prepared showing suitable properties.[80] In addition, the metal precursor availability and compatibility allow easy modification of the film stoichiometry and composition by atomic-scale precursor intermixing to fine tune the physical properties. Our group performed a meticulous study of the influence of cation substitution on BFO structure, morphology, optical and photoferroelectric properties from a metal–nitrate precursor solution deposited on (001) STO and processed at 550–650 °C under O_2 atmosphere.[81] Cobalt loads <30% ensured the formation of pure phase and epitaxial $BiFe_{1-x}Co_xO_3$ (BFCO) films with band gap modulation from 2.7 to 2.4 eV with improved photovoltaic performance while retaining the ferroelectric behavior. Larger cobalt concentrations, which are interesting to further tune the physical properties of BFCO,[82] resulted in the segregation of cobalt oxide phases. To improve the film quality and stability of these BFCO films, rare earth co-substitution was assessed as it helps minimizing bismuth volatilization and therefore the formation of defects.[83] Additions of 10% of lanthanum nitrate in BFCO precursor solution ensured the formation of reproducible epitaxial and pure phase La-BFCO films preserving the optical

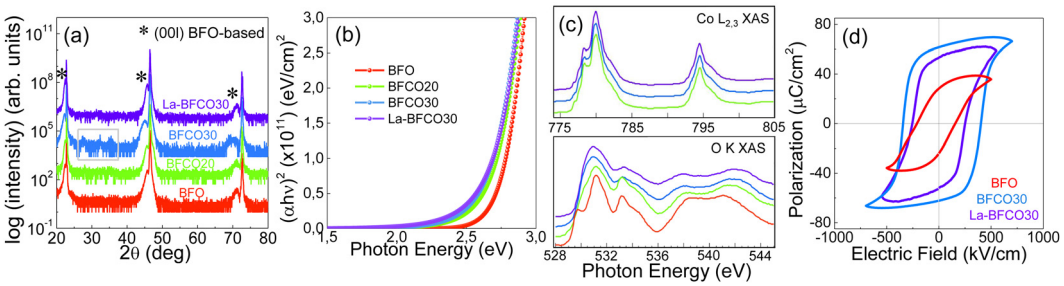

Fig. 3 Characterization of solution processed BFCO and La-doped BFCO thin films: (a) XRD θ–2θ scans – comparison of BFO, BFCO and La-BFCO films on STO; (b) Tauc plot extracted from ellipsometry measurements; (c) X-ray absorption spectroscopy measurements from Co $L_{2,3}$ edge and O K edge; (d) macroscopic ferroelectric loops measured at room temperature in a device configuration with Pt top contact and $La_{0.7}Sr_{0.3}MnO_3$ bottom contact. Reproduced from ref. 79 with permission from RSC, copyright 2021.

band gap and the ferroelectric properties.[79] X-ray absorption spectroscopy analysis supported by density functional theory revealed that the hybridization between Co 3d and O 2p determines the change in the optical bandgap being narrower with the coexistence of Co^{2+} and Co^{3+} oxidation states. The incorporation of La^{3+} did not affect the electronic structure or the optical properties (see Fig. 3). Therefore, the study put forward an attractive photoferroelectric material to be studied for unconventional photovoltaics, photo-detectors and opto-electronic devices.[84–86]

Overall, the CSD route allowed us to easily synthesize a wide variety of BFO chemical compositions and stoichiometries by simple metal–nitrate intermixing of up to four different precursors to obtain high quality and pure phase functional epitaxial films. On the other hand, the use of ALD to prepare BFO films, while doable, needs further investigation to exploit the superior capability of ALD to deliver uniform and conformal films and nanostructures with nanometer scale control of thickness and composition to facilitate the finest tuning of its multiferroic and photovoltaic properties.

Another fascinating area of research in the field of perovskite oxides is the search for non-toxic and element-abundant compositions that display simultaneous optical transparency and electrical conductivity to be used as transparent electrodes (TCO). Despite the high potential of CSD to process and engineer novel functional metal oxide materials with controlled composition, the preparation of perovskite-TCOs by CSD is at its infancy. There are few studies on n-type TCO films based on M-doped $BaSnO_3$ (M = La, Pr, Nd, Sb)[87,88] and also transparent and metallic La-doped $SrTiO_3$ thin films.[89] The development of p-type TCO is intrinsically more challenging. The localized nature of the O 2p orbitals at the top of the valence band of most metal oxides hinders the incorporation of shallow acceptors and large hole effective masses.[90,91] $La_{1-x}Sr_xCrO_3$ is a strong candidate with reasonably high transparency and p-type conductivity.[92] Therefore, motivated by this challenge, our recent contribution to this field was the development of a synthetic CSD procedure for p-type TCO $La_{0.75}Sr_{0.25}CrO_3$ (LSCO). We performed a thorough study on the influence of the solution chemistry based on metal nitrates to ultimately obtain epitaxial and reasonably smooth films on (001) STO and (001) $LaAlO_3$ (LAO) substrates.[93] The optimal formulation appeared to be nitrate precursors in 2-methoxyethanol, acetic acid and diethanolamine, processed in air which results in dense, epitaxial and slightly strained films. These LSCO films display 67% optical transparency in the visible spectrum being as good as those reported for some of the most promising state of the art TCOs.[94,95] The values of the electrical resistivity are roughly higher than those expected based on the film chemical doping and strain state and it is attributed to the presence of structural defects. Monochromated electron energy loss analysis allowed us to uniquely identify the formation of Cr^{4+} and a change in the hybridized orbitals Cr 3d–O 2p from the top of the valence band upon Sr-doping, which would be accountable for p-type conductivity. We envisage that this work will encourage new researchers to continue investigating the unprecedented class of p-type TCOs based on perovskites, and keep improving their physical properties to be ultimately integrated in the next generation transparent electronic, spintronic and energy storage and conversion devices.

Switching to spinel structure, $CoFe_2O_4$ (CFO) has stimulated considerable interest for its remarkable magnetic and electrochemical properties.[96,97] The cation distribution dramatically affects the properties and the deposition procedure has a key role in it.[98] The Co-rich ferrite phase is less investigated than the Fe-rich counterpart although it is predicted to show attractive magnetic, magneto-optic properties and photoelectrolysis activity.[99,100] In our group we evaluated the epitaxial stabilization at low temperature of the Co-rich ferrite by means of ALD.[50,101] Alternate pulsing of cobaltocene [$Co(Cp)_2$] and [$Fe(Cp)_2$] combined with ozone as the co-reactant at 250 °C delivered a series of epitaxial Co_2FeO_4 films from 5 to 25 nm thickness on both (001) and (110) oriented STO substrates.[50] High coercive fields, 15 kOe, and high saturation magnetization, 3.3 μ_B per formula unit, at 10 K were obtained for 10–25 nm films. Thinner films showed smaller saturation magnetization and a decrease in the coercive field because of the formation of antiphase boundaries.[102] Note that conformal coatings of Co_2FeO_4 on nanoporous structures can be easily achieved by ALD relying on the self-limiting surface reaction of the technique.[103] Overall, this study demonstrated that ALD is a suitable technique to stabilize by epitaxial growth complex oxide phases at low temperature by appropriate selection of

the precursor chemistry and lattice matched substrate. Soon after, other reports on the stabilization of metastable phases at low temperature of polycrystalline[104] and epitaxial[51] functional oxides were demonstrated by ALD.

Rare earth ferrite films, *e.g.* orthoferrite $GdFeO_3$ and garnet $Gd_3Fe_5O_{12}$, possess intriguing magnetic and magneto-optical properties[105,106] that can open new directions in the field of spintronics and magnonics.[107–111] The synthetic challenge for the $Gd_xFe_yO_z$ systems is to obtain pure-phase films to subsequently study the potential functional properties arising from the thin film itself and their interfaces.[3,112] Fabrication of $Gd_xFe_yO_z$ films by ALD remained unexplored. We attempted to prepare $Gd_xFe_yO_z$ systems using an ALD-type approach by first combining monometallic Gd and Fe precursors alternating Gd–O and Fe–O subcycles, see Fig. 4(a).[113] For that, tailor-made (tris(*N*,*N*′-diisopropyl-2-dimethylamido-guanidinato)gadolinium(III), $[Gd(DPDMG)_3]$[114] and bis(*N*-isopropyl ketoiminate)iron(II), $[Fe(^{i}pki)_2]$[115] were employed, together with ozone as a co-reactant to be deposited on both Si substrate and (001) STO substrates at 160–250 °C. The obtained films were compared with those deposited from commercial $[Fe(Cp)_2]$ and tailor-made $[Gd(DPDMG)_3]$. All obtained films were found with negligible amounts of organic species unveiled from Rutherford backscattering spectrometry. Interestingly, the tailor-made metalorganic precursors, designed to provide similar thermal behavior, resulted in the formation of polycrystalline $Gd_3Fe_5O_{12}$ films coexisting with $GdFeO_3$, Gd_2O_3 and Fe_2O_3 whereas the combination of $[Fe(Cp)_2]$ and $[Gd(DPDMG)_3]$ mainly favored the formation of $Gd_3Fe_5O_{12}$ films coexisting with traces of Gd_2O_3. The results further emphasize the influence of the metal–organic precursor composition to the final complex oxide film composition. An attractive approach to circumvent the complexity of searching for thermally compatible precursors is the use of heterobimetallic sources in which the cations of the targeted oxide are present in the starting metalorganic complex with the desired stoichiometry. Intrinsic advantages of bimetallic compounds include simplified precursor delivery, lowered deposition temperatures, retained stoichiometry and pre-defined chemical compatibility between the target film and the precursor.[55,59,117] For this, we showcased the epitaxial growth of $GdFeO_3$ films on (001) STO substrates by ALD using a volatile heterobimetallic Gd–Fe precursor $[GdFe(OtBu)_6(C_5H_5N)_2]$ containing Gd : Fe in the required stoichiometric ratio, with ozone as the co-reactant at 200 °C followed by post-treatment at 800 °C, see Fig. 4(b).[116] X-ray photoelectron spectroscopy confirmed close to nominal cation ratio (Fe : Gd = 0.9) with no N contamination, indicating successful cation transfer from the precursor and complete combustion of the ligands. Therefore, the combination of compatible chemistries with appropriate substrate interface energy helped promote epitaxial growth of stoichiometric films.

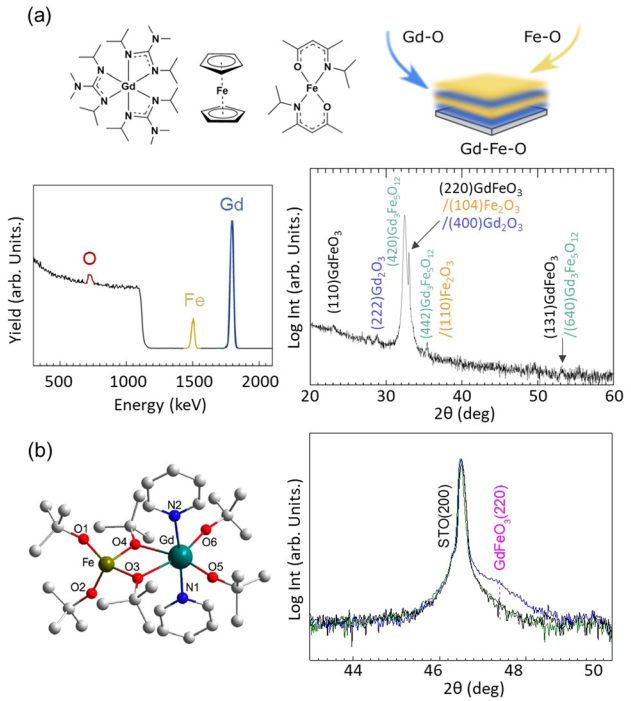

Fig. 4 Synthesis of $Gd_xFe_yO_z$ films: (a) combining monometallic Gd and Fe precursors *via* supercycles; (b) using a heterobimetallic single source precursor enabled epitaxial $GdFeO_3$ growth on $SrTiO_3$. Reproduced from ref. 113 and 116 with permission from RSC, copyright 2021 and Elsevier, copyright 2020.

4 Complex oxide freestanding membranes

The possibility of fabricating freestanding single crystal complex oxides has stimulated new research in synthetic procedures, investigating fundamental physics and envisaging a broader spectrum of applications for these materials.[17,20,118] The use of a sacrificial layer to obtain high-quality freestanding epitaxial complex oxide films is emerging as one of the most reliable fabrication methods. It consists in preparing an epitaxial sacrificial layer that induces the epitaxial growth of the complex oxide of interest and then be selectively etched to release the freestanding film. This process is quite challenging and involves identifying compatible materials in terms of structure, lattice mismatch and chemical reactivity, see Fig. 5. Several sacrificial layer compositions have been developed for the release of epitaxial complex oxide films.

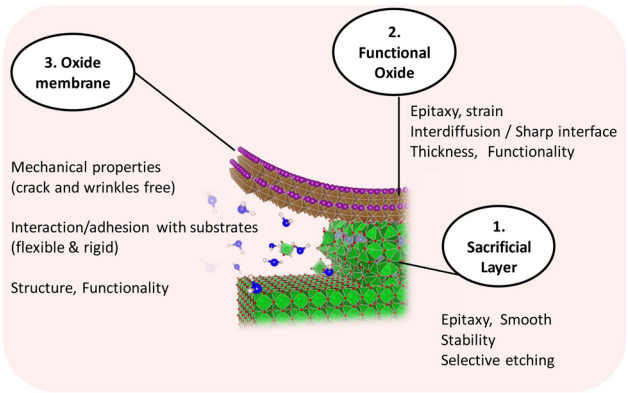

Fig. 5 Schematic of the challenges identified in each step of the preparation of a freestanding membrane from a sacrificial layer.

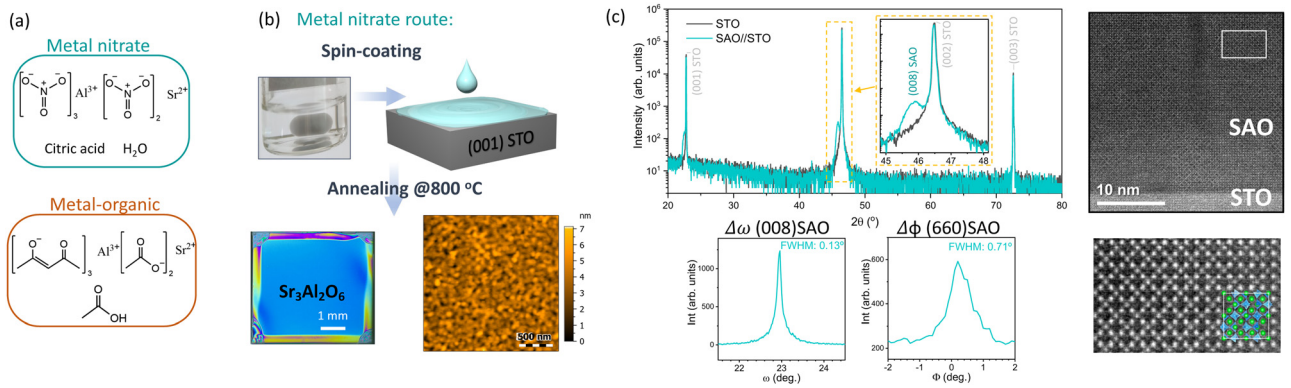

Fig. 6 Overview of the process to prepare epitaxial SAO films from solution processing. (a) Precursor choice, (b) deposition and annealing, and (c) structural characterization. Reproduced from ref. 142 with permission from Wiley, copyright 2021.

Some examples of sacrificial layers are $La_{0.7}Sr_{0.3}MnO_3$ (LSMO),[119–121] $SrRuO_3$,[122] $YBa_2Cu_3O_7$,[123] and $SrVO_3$[124] which have been used to release films with perovskite structures. Alternative structures such as brownmillerite $SrCoO_{2.5}$[125] or metal oxides with a rock salt structure including MgO[126] and BaO[127] have also demonstrated to fulfil the requirements to be used as a sacrificial layer for the release of epitaxial complex oxides of perovskites and spinels. The family of $Sr_{3-x}M_xAl_2O_6$ (M = Ba, Ca) has been the most studied and largely used sacrificial layer for the preparation of many different freestanding epitaxial complex oxides, which can be selectively etched with water. Despite its apparent structural complexity, $Sr_3Al_2O_6$ (SAO) shares a compatible lattice parameter with common perovskite oxides such as STO, a typical substrate used for the epitaxial growth of many functional perovskite oxide thin films. The SAO unit cell closely matches 4 unit cells of STO ($a_{SAO}/4$ = 3.961 Å; a_{STO} = 3.905 Å), with a mismatch of only 1%. Thanks to the resemblance in structure, single-phase epitaxially oriented SAO can be grown on STO.[128] The most typical perovskite oxide membranes prepared from SAO have been $BaTiO_3$,[129] $BiFeO_3$,[118,130] LSMO,[128] STO,[131,132] and $SrRuO_3$.[133] Nevertheless, the SAO sacrificial layer has also been proved useful to obtain other epitaxial oxide structures including spinels,[134,135] Fe_3O_4,[136] anatase TiO_2,[137] amorphous and polycrystalline oxides[138] and more complex designs such as heterostructures, superlattices[131,139] and vertically aligned nanostructures.[140,141] Notoriously, the fabrication of freestanding complex oxides has been mainly limited to the use of high-vacuum techniques such as PLD, MBE and sputtering. In order to provide a less-restrictive and more cost-efficient fabrication approach it is interesting to investigate how far can we go with chemical deposition approaches. In our group we investigated the use of CSD to prepare a water soluble SAO sacrificial layer by studying the viability of two different chemical formulations: metal nitrates *versus* metal–organics. A thorough study of the influence of precursor chemistry on gel decomposition and film quality allowed us to identify the metal nitrate precursor route as a robust approach to obtain epitaxial, dense and smooth SAO films (see Fig. 6).[142] Nonetheless, the ambient-exposure of the SAO sacrificial layer before depositing the complex oxide converts the top part of the epitaxial SAO film to amorphous.[143] Hence, subsequent ALD deposition of complex oxides such as $CoFe_2O_4$ (CFO) on this ambient-exposed CSD-SAO resulted in polycrystalline films.[143] From here, polycrystalline membranes can be obtained and they retain the characteristics of the film shown before the lift-off. For example, CFO membranes supported on a polymer are polycrystalline with a smooth surface (rms = 1 nm), and display similar saturation magnetization before and after the exfoliation, M_s = 150 emu cm^{-3} with coercivities of H_c = 0.7 kOe, Fig. 7. The obtained values of M_s are in line with those reported on epitaxial CFO membranes prepared from different approaches.[126,144–146] Attaching the membrane to kapton tape permits it to perform studies of the membrane held at different outward bending radii.[143]

This extreme SAO sensitivity to ambient humidity is a strong limitation for easy manipulation of the sacrificial layer in air

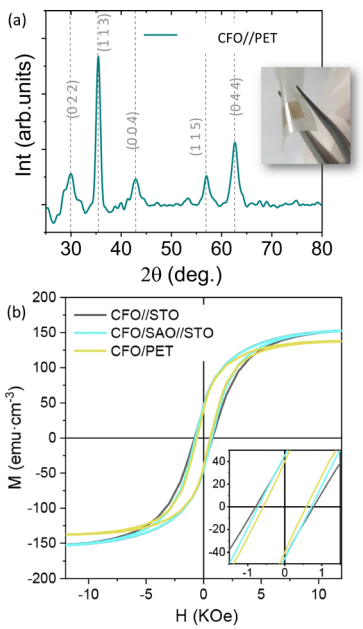

Fig. 7 ALD-CFO membranes on PET substrate (a) XRD θ–2θ scan and (b) $M(H)$ measurements at room temperature comparing CFO//STO, CFO/SAO//STO and CFO//PET. Reproduced from ref. 143 with permission from ACS, copyright 2022.

and restricted the deposition of epitaxial oxides to *in situ* approaches. Vacuum thermal annealing under an oxygen atmosphere can successfully recrystallize the SAO surface[143] and obtain epitaxial complex membranes,[147] but a more robust sacrificial layer would facilitate exploiting its full potential. Considering that the SAO fast hydrolysis is mostly determined by the ionicity of the Sr–O bond, performing cation nanoengineering in solution processed SAO, *i.e.* substituting Sr^{2+} by Ca^{2+}, can improve its ambient stability and also allow tuning the SAO lattice parameter from $a/4$ = 3.96 Å for $Sr_3Al_2O_6$ to $a/4$ = 3.81 Å for $Ca_3Al_2O_6$.[148]

Building on the versatility of CSD to perform cation engineering, we carried out a pioneering study of the influence of Ca-substitution on solution processed SAO ($Sr_{3-x}Ca_xAl_2O_6$, SCAO with $x \leq 3$) identifying an improvement in surface film crystallinity while preserving a smooth surface morphology. Notoriously, the SCAO films are more resistant to ambient degradation. For example, $SrCa_2Al_2O_6$ films exposed to air and sealed in bags under vacuum for two weeks preserved the surface crystallinity and smooth morphology. Therefore, the Ca-substitution favors the manipulation of the SAO sacrificial layer under less-restricted ambient conditions.[147]

Epitaxial LSMO films have been achieved on vacuum annealed SCAO sacrificial layers followed by the *in situ* deposition using PLD. We have observed that the quality of the SCAO, *i.e.* crystallinity and surface morphology (dictated by the Ca substitution) influences the properties of the LSMO grown on top.[147] The SCAO films with large Ca loads produces strained and biaxially textured LSMO films that upon lift-off result in a relaxed membrane with cracks and wrinkles. The electrical transport properties of the LSMO grown on SCAO are better than those of LSMO grown on pristine SAO and it is mostly attributed to the reduced cation interdiffusion between LSMO and SCAO. Finally, epitaxial and strain-free LSMO membranes exfoliated from SCAO and transferred on silicon or glass substrates show a metal–insulator transition at 290 K. Therefore, we demonstrate that CSD offers a facile route to deliver a series of sacrificial layer compositions by appropriate intermixing of chemical precursors and can deliver different complex oxides membranes including CFO, LSMO, and can be extended to many more opening new venues to study the behavior of these free-standing oxides.[147,149–151]

5 Conclusions

Cost-effective chemical deposition approaches are based on the appropriate combination of chemical precursors, and low or non-vacuum procedures allow easy tuning of the chemical composition of the films to tailor the film crystallinity, stability and physical properties. The richness of CSD relies on the easy combination of chemical precursors in a solution at ambient pressure to perform compositional engineering with high accuracy. Upon a well-controlled thermal treatment, epitaxial oxides with suitable properties were obtained. Pivoting on this versatility, cation-engineered and epitaxial BFCO, LSCO and SCAO compositions have been successfully prepared with remarkable structural and physical properties. This approach motivates to continue pursuing the development of new compositions to search for novel phenomena in oxides. The use of ALD has great potential to prepare epitaxial complex oxides at low temperature and perform conformal coatings as demonstrated for CFO films. The design of thermodynamically compatible precursors, monometallic and heterobimetallic, can broaden the range of feasible complex oxides prepared by ALD. Here we presented the case example of $Gd_xFe_yO_z$. Both techniques are envisaged to have a relevant role in the synthesis process of complex oxide membranes. Whereas CSD offers an easy way to prepare and tune complex oxide compositions, the precise thickness control in ALD down to the nanometer level will enable the synthesis and study of few monolayer thick complex oxide flexible membranes and manipulate their properties by means of strain.[18,19,138,152–154] A lot remains to be understood at the interface of complex oxides and the mechanical properties of the membranes. By the same token, it is foreseen that these chemical routes will contribute and speed up the design of artificial (and sharp) interface structures, stacking and twisting dissimilar materials, with almost atomic perfection. They can open new directions for high-performance oxide electronic and energy devices.

Author contributions

Pol Salles and Pamela Machado: methodology/study design; writing – original draft. Pengmei Yu: methodology/study design; writing – review editing. Mariona Coll: conceptualization; supervision; writing – review editing; funding acquisition.

Conflicts of interest

There are no conflicts to declare.

Acknowledgements

This work was funded by CEX2019-00917-S/MICIN/AEI/10.13039/501100011033 and PID2020-114224RB-I00/MICIN/AEI/10.13039/501100011033. We also acknowledge the financial support from the 2020 Leonardo grant for Researchers and Cultural Creators BBVA Foundation, the i-link A20346-CSIC project. The project that gave rise to these results received the support of a fellowship from the ''la Caixa'' Foundation (ID 100010434). The fellowship code is LCF/BQ/DI19/11730026. P. M. is grateful for financial support from the FPI fellowship (PRE2018-084618 MCIN/AEI/10.13039/5011000011033 by ESF invest in your future). We also acknowledge financial support from China Scholarship Council to P. Yu (201606920073). The work of P. M., P. S. and P. Y. has been done in the framework of the doctorate in Materials Science of the Autonomous University of Barcelona. We would like to acknowledge all the collaborators from those who provided novel metal precursors to the experts in thin film deposition and advanced characterization

and SUMAN group members who made the work presented in this Feature article possible.

Notes and references

1 F. Trier, P. Noël, J.-V. Kim, J.-P. Attané, L. Vila and M. Bibes, *Nat. Rev. Mater.*, 2022, **7**, 258–274.
2 T. Park, S. Deng, S. Manna, A. Islam-Nafiul, H. Yu, Y. Yuan, D. Fong, A. Chubykin, A. Sengupta, S. Sankaranarayanan and S. Ramanathan, *Adv. Mater.*, 2023, **35**, 2203352.
3 M. Coll, J. Fontcuberta, M. Althammer, M. Bibes, H. Boschker, A. Calleja, G. Cheng, M. Cuoco, R. Dittmann, B. Dkhil, I. El Baggari, M. Fanciulli, I. Fina, E. Fortunato, C. Frontera, S. Fujita, V. Garcia, S. Goennenwein, C.-G. Granqvist, J. Grollier, R. Gross, A. Hagfeldt, G. Herranz, K. Hono, E. Houwman, M. Huijben, A. Kalaboukhov, D. Keeble, G. Koster, L. Kourkoutis, J. Levy, M. Lira-Cantu, J. MacManus-Driscoll, J. Mannhart, R. Martins, S. Menzel, T. Mikolajick, M. Napari, M. Nguyen, G. Niklasson, C. Paillard, S. Panigrahi, G. Rijnders, F. Sánchez, P. Sanchis, S. Sanna, D. Schlom, U. Schroeder, K. Shen, A. Siemon, M. Spreitzer, H. Sukegawa, R. Tamayo, J. van den Brink, N. Pryds and F. M. Granozio, *Appl. Surf. Sci.*, 2019, **482**, 1–93.
4 J. L. MacManus-Driscoll, M. P. Wells, C. Yun, J.-W. Lee, C.-B. Eom and D. G. Schlom, *APL Mater.*, 2020, **8**, 040904.
5 G. Koster, M. Huijben, A. Janssen and G. Rijnders, *Epitaxial Growth of Complex Metal Oxides*, Elsevier, 2015, pp. 3–29.
6 W. Li, J. Shi, K. H. L. Zhang and J. L. MacManus-Driscoll, *Mater. Horiz.*, 2020, **7**, 2832–2859.
7 *Pulsed Laser Deposition of Thin Films: Applications-Led Growth of Functional Materials*, ed. R. Eason, Wiley, 2006.
8 M. Spreitzer, D. Klement, T. Parkelj Potočnik, U. Trstenjak, Z. Jovanović, M. D. Nguyen, H. Yuan, J. E. ten Elshof, E. Houwman, G. Koster, G. Rijnders, J. Fompeyrine, L. Kornblum, D. P. Fenning, Y. Liang, W.-Y. Tong and P. Ghosez, *APL Mater.*, 2021, **9**, 040701.
9 D. G. Schlom, *APL Mater.*, 2015, **3**, 062403.
10 *Epitaxial Growth of Complex Metal Oxides*, ed. G. Koster, M. Huijben and G. Rijnders, Woodhead Publishing, 2022.
11 J. L. MacManus-Driscoll, M. Bianchetti, A. Kursumovic, G. Kim, W. Jo, H. Wang, J. H. Lee, G. W. Hong and S. H. Moon, *APL Mater.*, 2014, **2**, 086103.
12 R. W. Schwartz, *Mater. Sci.*, 1997, **9**, 2325–2340.
13 J. M. Vila-Fungueiriño, B. Rivas-Murias, J. Rubio-Zuazo, A. Carretero-Genevrier, M. Lazzari and F. Rivadulla, *J. Mater. Chem. C*, 2018, **6**, 3834–3844.
14 M. Coll and M. Napari, *APL Mater.*, 2019, **7**, 110901.
15 J. M. Vila-Fungueiriño, R. Bachelet, G. Saint-Girons, M. Gendry, M. Gich, J. Gazquez, E. Ferain, F. Rivadulla, J. Rodriguez-Carvajal and N. Mestres, *et al.*, *Front. Phys.*, 2015, **3**, 38.
16 E. A. Cochran, K. N. Woods, D. W. Johnson, C. J. Page and S. W. Boettcher, *J. Mater. Chem. A*, 2019, **7**, 24124–24149.
17 F. M. Chiabrera, S. Yun, Y. Li, R. T. Dahm, H. Zhang, C. K. R. Kirchert, D. V. Christensen, F. Trier, T. S. Jespersen and N. Pryds, *Ann. Phys.*, 2022, **534**, 2200084.
18 H. S. Kum, H. Lee, S. Kim, S. Lindemann, W. Kong, K. Qiao, P. Chen, J. Irwin, J. H. Lee, S. Xie, S. Subramanian, J. Shim, S.-H. Bae, C. Choi, L. Ranno, S. Seo, S. Lee, J. Bauer, H. Li, K. Lee, J. A. Robinson, C. A. Ross, D. G. Schlom, M. S. Rzchowski, C.-B. Eom and J. Kim, *Nature*, 2020, **578**, 75–81.
19 L. Dai, F. An, J. Zou, X. Zhong and G. Zhong, *J. Appl. Phys.*, 2022, **132**, 070904.
20 D. Pesquera, A. Fernández, E. Khestanova and L. W. Martin, *J. Phys.: Condens. Matter*, 2022, **34**, 383001.
21 C. Brinker and G. W. Scherer, *Sol-Gel Science. The Physics and Chemistry of Sol-Gel Processing*, Elsevier, E. I. du Pont de Nemours Company, Wilmington, Delaware, 1990.
22 S. A. Chambers, *Surf. Sci. Rep.*, 2000, **39**, 105–180.
23 H. Kozuka, in *Sol-Gel Preparation of Crystalline Oxide Thin Films on Plastics*, ed. L. Klein, M. Aparicio and A. Jitianu, Springer International Publishing, Cham, 2016, pp. 1–24.
24 I. Bretos, R. Jiménez, J. Ricote and M. L. Calzada, *Chem. Soc. Rev.*, 2018, **47**, 291–308.
25 C. Lin, Z. Zhang, Z. Dai, M. Wu, S. Liu, J. Chen, C. Hua, Y. Lu, F. Zhang and H. Lou, *et al.*, *Nat. Commun.*, 2023, **14**, 2341.
26 Y. K. Lee, C. J. Kim, J. K. Lee, I. Yi, I. Chung and W. Lee, *Integr. Ferroelectr.*, 2001, **41**, 175–183.
27 P. Lin, W. Ren, X. Wu, P. Shi, X. Chen and X. Yao, *Ceram. Int.*, 2008, **34**, 991–995.
28 B. Villarejo, F. Pino, C. Pop, S. Ricart, F. Vallès, B. Mundet, A. Palau, P. Roura-Grabulosa, J. Farjas, N. Chamorro, R. Yáñez, X. Granados, T. Puig and X. Obradors, *ACS Appl. Electron. Mater.*, 2021, **3**, 3948–3961.
29 M. Coll, R. Guzman, P. Garcés, J. Gazquez, V. Rouco, A. Palau, S. Ye, C. Magen, H. Suo, H. Castro, T. Puig and X. Obradors, *Supercond. Sci. Technol.*, 2014, **27**, 044008.
30 Z. Li, M. Coll, B. Mundet, N. Chamorro, F. Vallès, A. Palau, J. Gazquez, S. Ricart, T. Puig and X. Obradors, *Sci. Rep.*, 2019, **9**, 5828.
31 K. De Keukeleere, P. Cayado, A. Meledin, F. Vallès, J. De Roo, H. Rijckaert, G. Pollefeyt, E. Bruneel, A. Palau, M. Coll, S. Ricart, G. Van Tendeloo, T. Puig, X. Obradors and I. Van Driessche, *Adv. Electron. Mater.*, 2016, **2**, 1600161.
32 A. Carretero-Genevrier, T. Puig, X. Obradors and N. Mestres, *Chem. Soc. Rev.*, 2014, **43**, 2042–2054.
33 X. Obradors, T. Puig, M. Gibert, A. Queraltó, J. Zabaleta and N. Mestres, *Chem. Soc. Rev.*, 2014, **43**, 2200.
34 M. Ritala and M. Leskelä, *Handbook of Thin Films*, Elsevier, 2002, pp. 103–159.
35 P. Poodt, J. van Lieshout, A. Illiberi, R. Knaapen, F. Roozeboom and A. van Asten, *J. Vac. Sci. Technol., A*, 2013, **31**, 01A108.
36 V. Cremers, R. L. Puurunen and J. Dendooven, *Appl. Phys. Rev.*, 2019, **6**, 021302.
37 D. Muñoz-Rojas and J. MacManus-Driscoll, *Mater. Horiz.*, 2014, **1**, 314–320.
38 D. Muñoz-Rojas, V. H. Nguyen, C. Masse de la Huerta, S. Aghazadehchors, C. Jiménez and D. Bellet, *C. R. Phys.*, 2017, **18**, 391–400.
39 A. J. M. Mackus, M. J. M. Merkx and W. M. M. Kessels, *Chem. Mater.*, 2019, **31**, 2–12.
40 G. N. Parsons and R. D. Clark, *Chem. Mater.*, 2020, **32**, 4920–4953.
41 L. Hu, W. Qi and Y. Li, *Nanotechnol. Rev.*, 2017, **6**, 527–547.
42 C. Marichy, M. Bechelany and N. Pinna, *Adv. Mater.*, 2012, **24**, 1017–1032.
43 E. Granneman, P. Fischer, D. Pierreux, H. Terhorst and P. Zagwijn, *Surf. Coat. Technol.*, 2007, **201**, 8899–8907.
44 K. Sharma, R. A. Hall and S. M. George, *J. Vac. Sci. Technol.*, 2015, **33**, 01A132.
45 M. Ritala, K. Kukli, A. Rahtu, P. I. Räisänen, M. Leskelä, T. Sajavaara and J. Keinonen, *Science*, 2000, **288**, 319–321.
46 A. Devi, *Coord. Chem. Rev.*, 2013, **257**, 3332–3384.
47 A. J. M. Mackus, J. R. Schneider, C. MacIsaac, J. G. Baker and S. F. Bent, *Chem. Mater.*, 2019, **31**, 1142–1183.
48 E. Ahvenniemi, M. Matvejeff and M. Karppinen, *Dalton Trans.*, 2015, **44**, 8001–8006.
49 H. H. Sønsteby, E. Skaar, H. FjellvÅg and O. Nilsen, *ACS Appl. Electron. Mater.*, 2021, **3**, 292–298.
50 M. Coll, J. M. Montero Moreno, J. Gazquez, K. Nielsch, X. Obradors and T. Puig, *Adv. Funct. Mater.*, 2014, **24**, 5368–5374.
51 H. H. Sønsteby, E. Skaar, Ø. S. Fjellvåg, J. E. Bratvold, H. Fjellvåg and O. Nilsen, *Nat. Commun.*, 2020, **11**, 2872.
52 M. Vehkamäki, T. Hatanpää, M. Ritala, M. Leskelä, S. Väyrynen and E. Rauhala, *Chem. Vap. Deposition*, 2007, **13**, 239–246.
53 Y. Gao, O. Zandi and T. W. Hamann, *J. Mater. Chem. A*, 2016, **4**, 2826–2830.
54 O. Nilsen, E. Rauwel, H. FjellvÅg and A. Kjekshus, *J. Mater. Chem.*, 2007, **17**, 1466–1475.
55 T. Hatanpää, M. Ritala and M. Leskelä, *Coord. Chem. Rev.*, 2013, **257**, 3297–3322.
56 M. Vehkamäki, M. Ritala, M. Leskelä, A. C. Jones, H. O. Davies, T. Sajavaara and E. Rauhala, *J. Electrochem. Soc.*, 2004, **151**, F69.
57 J. M. Gaskell, S. Przybylak, A. C. Jones, H. C. Aspinall, P. R. Chalker, K. Black, R. J. Potter, P. Taechakumput and S. Taylor, *Chem. Mater.*, 2007, **19**, 4796–4803.
58 J. Harjuoja, T. Hatanpää, M. Vehkamäki, S. Väyrynen, M. Putkonen, L. Niinistö, M. Ritala, M. Leskelä and E. Rauhala, *Chem. Vap. Deposition*, 2005, **11**, 362–367.

59 P. Marchand and C. J. Carmalt, *Coord. Chem. Rev.*, 2013, **257**, 3202–3221.
60 K. Bernal Ramos, M. J. Saly and Y. J. Chabal, *Coord. Chem. Rev.*, 2013, **257**, 3271–3281.
61 N. E. Richey, C. de Paula and S. F. Bent, *J. Chem. Phys.*, 2020, **152**, 040902.
62 F. Zavaliche, S. Y. Yang, T. Zhao, Y. H. Chu, M. P. Cruz, C. B. Eom and R. Ramesh, *Phase Transitions*, 2006, **79**, 991–1017.
63 S. Y. Yang, J. Seidel, S. J. Byrnes, P. Shafer, C.-H. Yang, M. D. Rossell, P. Yu, Y.-H. Chu, J. F. Scott, J. W. Ager, L. W. Martin and R. Ramesh, *Nat. Nanotechnol.*, 2010, **5**, 143–147.
64 S. M. Young, F. Zheng and A. M. Rappe, *Phys. Rev. Lett.*, 2012, **109**, 236601.
65 T. Rojac, A. Bencan, B. Malic, G. Tutuncu, J. L. Jones, J. E. Daniels and D. Damjanovic, *J. Am. Ceram. Soc.*, 2014, **97**, 1993–2011.
66 S. M. Selbach, M.-A. Einarsrud and T. Grande, *Chem. Mater.*, 2009, **21**, 169–173.
67 E. M. Levin and R. S. Roth, *J. Res. Natl. Bur. Stand.*, 1964, **68**, 197–206.
68 M. I. Morozov, N. A. Lomanova and V. V. Gusarov, *Russ. J. Gen. Chem.*, 2003, **73**, 1676–1680.
69 C. Ederer and N. A. Spaldin, *Phys. Rev. B: Condens. Matter Mater. Phys.*, 2005, **71**, 224103.
70 A. Maitre, M. Francois and J. Gachon, *J. Phase Equilib. Diffus.*, 2004, **25**, 59–67.
71 Q. Zhang, D. Sando and V. Nagarajan, *J. Mater. Chem. C*, 2016, **4**, 4092–4124.
72 M. Valant, A.-K. Axelsson and N. Alford, *Chem. Mater.*, 2007, **19**, 5431–5436.
73 F. Zhang, G. Sun, W. Zhao, L. Wang, L. Zheng, S. Liu, B. Liu, L. Dong, X. Liu, G. Yan, L. Tian and Y. Zeng, *J. Phys. Chem. C*, 2013, **117**, 24579–24585.
74 A. R. Akbashev, G. Chen and J. E. Spanier, *Nano Lett.*, 2014, **14**, 44–49.
75 M. Coll, J. Gazquez, I. Fina, Z. Khayat, A. Quindeau, M. Alexe, M. Varela, S. Trolier-McKinstry, X. Obradors and T. Puig, *Chem. Mater.*, 2015, **27**, 6322–6328.
76 M. J. Müller, K. Komander, C. Höhn, R. van de Krol and A. C. Bronneberg, *ACS Appl. Nano Mater.*, 2019, **2**, 6277–6286.
77 T. J. Knisley, L. C. Kalutarage and C. H. Winter, *Coord. Chem. Rev.*, 2013, **257**, 3222–3231.
78 S. Kang and S. Rhee, *Thin Solid Films*, 2004, **468**, 79–83.
79 P. Machado, I. Caño, C. Menéndez, C. Cazorla, H. Tan, I. Fina, M. Campoy-Quiles, C. Escudero, M. Tallarida and M. Coll, *J. Mater. Chem. C*, 2021, **9**, 330–339.
80 B. Yang, L. Jin, R. Wei, X. Tang, L. Hu, P. Tong, J. Yang, W. Song, J. Dai, X. Zhu, Y. Sun, S. Zhang, X. Wang and Z. Cheng, *Small*, 2021, **17**, 1903663.
81 P. Machado, M. Scigaj, J. Gazquez, E. Rueda, A. Sánchez-Díaz, I. Fina, M. Gibert-Roca, T. Puig, X. Obradors, M. Campoy-Quiles and M. Coll, *Chem. Mater.*, 2019, **31**, 947–954.
82 O. Diéguez and J. Íñiguez, *Phys. Rev. Lett.*, 2011, **107**, 057601.
83 Z. X. Cheng, A. H. Li, X. L. Wang, S. X. Dou, K. Ozawa, H. Kimura, S. J. Zhang and T. R. Shrout, *J. Appl. Phys.*, 2008, **103**, 07E507.
84 C. Paillard, X. Bai, I. C. Infante, M. Guennou, G. Geneste, M. Alexe, J. Kreisel and B. Dkhil, *Adv. Mater.*, 2016, **28**, 5153–5168.
85 P. Lopez-Varo, L. Bertoluzzi, J. Bisquert, M. Alexe, M. Coll, J. Huang, J. A. Jimenez-Tejada, T. Kirchartz, R. Nechache, F. Rosei and Y. Yuan, *Phys. Rep.*, 2016, **653**, 1–40.
86 P. Machado, P. Salles, A. Frebel, G. De Luca, E. Ros, I. Fina, J. Puigdollers and M. Coll, submitted, 2023.
87 R. Wei, X. Tang, L. Hu, X. Luo, J. Yang, W. Song, J. Dai, X. Zhu and Y. Sun, *ACS Appl. Energy Mater.*, 2018, **1**, 1585–1593.
88 R. H. Wei, L. Hu, C. Shao, X. W. Tang, X. Luo, J. M. Dai, J. Yang, W. H. Song, X. B. Zhu and Y. P. Sun, *Appl. Phys. Lett.*, 2019, **115**, 162105.
89 X. Zhu, S. Zhang, H. Lei, X. Zhu, G. Li, B. Wang, W. Song, Z. Yang, J. Dai, Y. Sun, D. Shi and S. Dou, *J. Am. Ceram. Soc.*, 2009, **92**, 800–804.
90 L. Zhang, Y. Zhou, L. Guo, W. Zhao, A. Barnes, H.-T. F. J. Zhang, C. Eaton, Y. Zheng, M. Brahlek, H. F. Haneef, N. J. Podraza, M. H. W. Chan, V. Gopalan, K. M. Rabe and R. Engel-Herbert, *Nat. Mater.*, 2016, **15**, 1–8.
91 D. D. Sarma, K. Maiti, E. Vescovo, C. Carbone, W. Eberhardt, O. Rader and W. Gudat, *Phys. Rev. B: Condens. Matter Mater. Phys.*, 1996, **53**, 13369–13373.
92 K. H. L. Zhang, Y. Du, A. Papadogianni, O. Bierwagen, S. Sallis, L. F. J. Piper, M. E. Bowden, V. Shutthanandan, P. V. Sushko and S. A. Chambers, *Adv. Mater.*, 2015, **27**, 5191–5195.
93 P. Machado, R. Guzmán, R. J. Morera, J. Alcalà, A. Palau, W. Zhou and M. Coll, *Chem. Mater.*, 2023, **35**, 3513–3521.
94 A. Stadler, *Materials*, 2012, **5**, 661–683.
95 E. Fortunato, D. Ginley, H. Hosono and D. C. Paine, *MRS Bull.*, 2007, **32**, 242–247.
96 F. Eskandari, S. B. Porter, M. Venkatesan, P. Kameli, K. Rode and J. M. D. Coey, *Phys. Rev. Mater.*, 2017, **1**, 074413.
97 Q. He, K. Rui, C. Chen, J. Yang and Z. Wen, *ACS Appl. Mater. Interfaces*, 2017, **9**, 36927–36935.
98 G. P. Gardner, Y. B. Go, D. M. Robinson, P. F. Smith, J. Hadermann, A. Abakumov, M. Greenblatt and G. C. Dismukes, *Angew. Chem., Int. Ed.*, 2012, **51**, 1616–1619.
99 A. Walsh, S.-H. Wei, Y. Yan, M. M. Al-Jassim, J. A. Turner, M. Woodhouse and B. A. Parkinson, *Phys. Rev. B: Condens. Matter Mater. Phys.*, 2007, **76**, 165119.
100 P. A. Salvador, T.-D. Doan, B. Mercey and B. Raveau, *Chem. Mater.*, 1998, **10**, 2592–2595.
101 M. Coll, J. Gazquez, A. Palau, M. Varela, X. Obradors and T. Puig, *Chem. Mater.*, 2012, **24**, 3732–3737.
102 J.-B. Moussy, *J. Phys. D: Appl. Phys.*, 2013, **46**, 143001.
103 J. Zhang, M. Coll, T. Puig, E. Pellicer and J. Sort, *J. Mater. Chem. C*, 2016, **4**, 8655–8662.
104 Y. Zhang, M. Liu, Y. Zhang, X. Chen, W. Ren and Z.-G. Ye, *J. Appl. Phys.*, 2015, **117**, 17C743.
105 S. Geller, *J. Chem. Phys.*, 1956, **24**, 1236–1239.
106 M. A. Gilleo, *J. Chem. Phys.*, 1956, **24**, 1239–1243.
107 Y. Tokunaga, N. Furukawa, H. Sakai, Y. Taguchi, T. H. Arima and Y. Tokura, *Nat. Mater.*, 2009, **8**, 558–562.
108 A. Panchwanee, V. Raghavendra Reddy, A. Gupta, R. Choudhary, D. Phase and V. Ganesan, *Thin Solid Films*, 2019, **669**, 301–305.
109 E. E. Anderson, J. R. Cunningham and G. E. McDuffie, *Phys. Rev.*, 1959, **116**, 624–625.
110 Y. Tokunaga, Y. Taguchi, T.-H. Arima and Y. Tokura, *Nat. Phys.*, 2012, **8**, 838–844.
111 A. A. Serga, A. V. Chumak and B. Hillebrands, *J. Phys. D: Appl. Phys.*, 2010, **43**, 264002.
112 M. Bibes, J. E. Villegas and A. Barthélémy, *Adv. Phys.*, 2011, **60**, 5–84.
113 P. Yu, S. M. J. Beer, A. Devi and M. Coll, *CrystEngComm*, 2021, **23**, 730–740.
114 A. P. Milanov, R. A. Fischer and A. Devi, *Inorg. Chem.*, 2008, **47**, 11405–11416.
115 D. Peeters, A. Sadlo, K. Lowjaga, O. Mendoza Reyes, L. Wang, L. Mai, M. Gebhard, D. Rogalla, H.-W. Becker, I. Giner, G. Grundmeier, D. Mitoraj, M. Grafen, A. Ostendorf, R. Beranek and A. Devi, *Adv. Mater. Interfaces*, 2017, **4**, 1700155.
116 S. Mathur, M. Veith, H. Shen, S. Hüfner and M. H. Jilavi, *Chem. Mater.*, 2002, **14**, 568–582.
117 C. Bohr, P. Yu, M. Scigaj, C. Hegemann, T. Fischer, M. Coll and S. Mathur, *Thin Solid Films*, 2020, **698**, 137848.
118 D. Ji, S. Cai, T. R. Paudel, H. Sun, C. Zhang, L. Han, Y. Wei, Y. Zang, M. Gu, Y. Zhang, W. Gao, H. Huyan, W. Guo, D. Wu, Z. Gu, E. Y. Tsymbal, P. Wang, Y. Nie and X. Pan, *Nature*, 2019, **570**, 87–90.
119 S. R. Bakaul, C. R. Serrao, M. Lee, C. W. Yeung, A. Sarker, S.-L. Hsu, A. K. Yadav, L. Dedon, L. You, A. I. Khan, J. D. Clarkson, C. Hu, R. Ramesh and S. Salahuddin, *Nat. Commun.*, 2016, **7**, 10547.
120 S. Puebla, T. Pucher, V. Rouco, G. Sanchez-Santolino, Y. Xie, V. Zamora, F. A. Cuellar, F. J. Mompean, C. Leon, J. O. Island, M. Garcia-Hernandez, J. Santamaria, C. Munuera and A. Castellanos-Gomez, *Nano Lett.*, 2022, **22**, 7457–7466.
121 D. Pesquera, E. Parsonnet, A. Qualls, R. Xu, A. J. Gubser, J. Kim, Y. Jiang, G. Velarde, Y. Huang, H. Y. Hwang, R. Ramesh and L. W. Martin, *Adv. Mater.*, 2020, **32**, 2003780.
122 D. Pesquera, E. Khestanova, M. Ghidini, S. Zhang, A. P. Rooney, F. Maccherozzi, P. Riego, S. Farokhipoor, J. Kim, X. Moya, M. E. Vickers, N. A. Stelmashenko, S. J. Haigh, S. S. Dhesi and N. D. Mathur, *Nat. Commun.*, 2020, **11**, 3190.
123 Y.-W. Chang, P.-C. Wu, J.-B. Yi, Y.-C. Liu, Y. Chou, Y.-C. Chou and J.-C. Yang, *Nanoscale Res. Lett.*, 2020, **15**, 172.

124 Y. Bourlier, B. Bérini, M. Frégnaux, A. Fouchet, D. Aureau and Y. Dumont, *ACS Appl. Mater. Interfaces*, 2020, **12**, 8466–8474.
125 H. Peng, N. Lu, S. Yang, Y. Lyu, Z. Liu, Y. Bu, S. Shen, M. Li, Z. Li, L. Gao, S. Lu, M. Wang, H. Cao, H. Zhou, P. Gao, H. Chen and P. Yu, *Adv. Funct. Mater.*, 2022, 2111907.
126 Y. Zhang, L. Shen, M. Liu, X. Li, X. Lu, L. Lu, C. Ma, C. You, A. Chen, C. Huang, L. Chen, M. Alexe and C.-L. Jia, *ACS Nano*, 2017, **11**, 8002–8009.
127 R. Takahashi and M. Lippmaa, *ACS Appl. Mater. Interfaces*, 2020, **12**, 25042–25049.
128 Z. Lu, J. Liu, J. Feng, X. Zheng, L.-H. Yang, C. Ge, K.-J. Jin, Z. Wang and R.-W. Li, *APL Mater.*, 2020, **8**, 051105.
129 H. Sun, J. Wang, Y. Wang, C. Guo, J. Gu, W. Mao, J. Yang, Y. Liu, T. Zhang, T. Gao, H. Fu, T. Zhang, Y. Hao, Z. Gu, P. Wang, H. Huang and Y. Nie, *Nat. Commun.*, 2022, **13**, 4332.
130 B. Peng, R.-C. Peng, Y.-Q. Zhang, G. Dong, Z. Zhou, Y. Zhou, T. Li, Z. Liu, Z. Luo, S. Wang, Y. Xia, R. Qiu, X. Cheng, F. Xue, Z. Hu, W. Ren, Z.-G. Ye, L.-Q. Chen, Z. Shan, T. Min and M. Liu, *Sci. Adv.*, 2020, **6**, eaba5847.
131 D. Lu, D. J. Baek, S. S. Hong, L. F. Kourkoutis, Y. Hikita and H. Y. Hwang, *Nat. Mater.*, 2016, **15**, 1255–1260.
132 S. S. Hong, J. H. Yu, D. Lu, A. F. Marshall, Y. Hikita, Y. Cui and H. Y. Hwang, *Sci. Adv.*, 2017, **3**, eaao5173.
133 Z. Lu, Y. Yang, L. Wen, J. Feng, B. Lao, X. Zheng, S. Li, K. Zhao, B. Cao, Z. Ren, D. Song, H. Du, Y. Guo, Z. Zhong, X. Hao, Z. Wang and R.-W. Li, *npj Flexible Electron.*, 2022, **6**, 9.
134 M. Yao, Y. Li, B. Tian, Q. Mao, G. Dong, Y. Cheng, W. Hou, Y. Zhao, T. Wang, Y. Zhao, Z. Jiang, M. Liu and Z. Zhou, *J. Mater. Chem. C*, 2020, **8**, 17099–17106.
135 T. Wang, G. Dong, Y. Ma, H. Liu, Z. Zhou and M. Liu, *J. Materiomics*, 2022, **8**, 596–600.
136 W. Hou, M. Yao, R. Qiu, Z. Wang, Z. Zhou, K. Shi, J. Pan, M. Liu and J. Hu, *J. Alloys Compd.*, 2021, **887**, 161470.
137 A. Hiraoka, K. Fujiwara and H. Nishikawa, *Electron. Commun. Jpn.*, 2021, **104**, 767–770.
138 L. Zhang, D. Zhang, L. Jin, B. Liu, H. Meng, X. Tang, M. Li, S. Liu, Z. Zhong and H. Zhang, *APL Mater.*, 2021, **9**, 061105.
139 Y. Li, E. Zatterin, M. Conroy, A. Pylypets, F. Borodavka, A. Björling, D. J. Groenendijk, E. Lesne, A. J. Clancy, M. Hadjimichael, D. Kepaptsoglou, Q. M. Ramasse, A. D. Caviglia, J. Hlinka, U. Bangert, S. J. Leake and P. Zubko, *Adv. Mater.*, 2022, **34**, 2106826.
140 J. Huang, D. Zhang, J. Liu and H. Wang, *Mater. Res. Lett.*, 2022, **10**, 287–294.
141 G. Zhong, F. An, K. Qu, Y. Dong, Z. Yang, L. Dai, S. Xie, R. Huang, Z. Luo and J. Li, *Small*, 2021, 2104213.
142 P. Salles, I. Caño, R. Guzman, C. Dore, A. Mihi, W. Zhou and M. Coll, *Adv. Mater. Interfaces*, 2021, **8**, 2001643.
143 P. Salles, R. Guzmán, D. Zanders, A. Quintana, I. Fina, F. Sánchez, W. Zhou, A. Devi and M. Coll, *ACS Appl. Mater. Interfaces*, 2022, **14**, 12845–12854.
144 H. Kum, D. Lee, W. Kong, H. Kim, Y. Park, Y. Kim, Y. Baek, S.-H. Bae, K. Lee and J. Kim, *Nat. Electron.*, 2019, **2**, 439–450.
145 H.-J. Liu, C.-K. Wang, D. Su, T. Amrillah, Y.-H. Hsieh, K.-H. Wu, Y.-C. Chen, J.-Y. Juang, L. M. Eng, S.-U. Jen and Y.-H. Chu, *ACS Appl. Mater. Interfaces*, 2017, **9**, 7297–7304.
146 K. L. Oh, Y. M. Kwak, D. S. Kong, S. Ryu, H. Kim, H. Jeen, S. Choi and J. H. Jung, *Curr. Appl. Phys.*, 2021, **31**, 87–92.
147 P. Salles, R. Guzmán, A. Barrera, M. Ramis, J. M. Caceido, A. Palau, W. Zhou and M. Coll, *Adv. Funct. Mater.*, 2023, 2304059.
148 A. Prodjosantoso, B. J. Kennedy and B. A. Hunter, *Aust. J. Chem.*, 2000, **53**, 195–202.
149 P. Singh, A. Swartz, D. Lu, S. S. Hong, K. Lee, A. F. Marshall, K. Nishio, Y. Hikita and H. Y. Hwang, *ACS Appl. Electron. Mater.*, 2019, **1**, 1269–1274.
150 S. S. Hong, M. Gu, M. Verma, V. Harbola, B. Y. Wang, D. Lu, A. Vailionis, Y. Hikita, R. Pentcheva, J. M. Rondinelli and H. Y. Hwang, *Science*, 2020, **368**, 71–76.
151 R. Xu, J. Huang, E. S. Barnard, S. S. Hong, P. Singh, E. K. Wong, T. Jansen, V. Harbola, J. Xiao, B. Y. Wang, S. Crossley, D. Lu, S. Liu and H. Y. Hwang, *Nat. Commun.*, 2020, **11**, 3141.
152 J. Karthik, J. C. Agar, A. R. Damodaran and L. W. Martin, *Phys. Rev. Lett.*, 2012, **109**, 257602.
153 S. Das, Y. Tang, Z. Hong, M. Gonçalves, M. McCarter, C. Klewe, K. Nguyen, F. Gómez-Ortiz, P. Shafer, E. Arenholz, V. Stoica, S. Hsy, C. Ophus, J. Liu, C. Nelson, S. Saremi, B. Prasad, A. Mei, D. Schlom, J. Íñiguez, P. Garcia-Fernández, D. Muller, L. Chen, J. Junquera, L. Martin and R. Ramesh, *Nature*, 2019, **568**, 368–372.
154 Q. Lu, Q. Wang, Q. Yang, L. Cheng and X. Zhai, *Appl. Phys. Lett.*, 2022, **121**, 171601.

